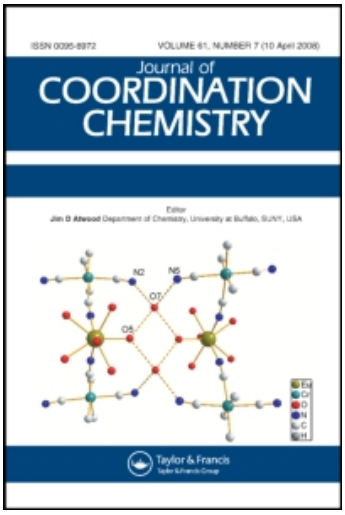

Journal of Coordination Chemistry
Publication details, including instructions for authors and subscription information:
http://www.informaworld.com/smpp/title~content=t713455674

Structural Aspects of the Dephosphorylation of Adenosine Triphosphate Catalyzed by Polyammonium Macrocycles

Ligang Qian[a]; Zhong Sun[a]; Jinnian Gao[a]; Barahman Movassagh[a]; Luis Morales[a]; Kristin Bowman Mertes[a]
[a] Departments of Chemistry and Medicinal Chemistry, University of Kansas, Lawrence, Kansas, USA

To cite this Article Qian, Ligang , Sun, Zhong , Gao, Jinnian , Movassagh, Barahman , Morales, Luis and Mertes, Kristin Bowman(1991) 'Structural Aspects of the Dephosphorylation of Adenosine Triphosphate Catalyzed by Polyammonium Macrocycles', Journal of Coordination Chemistry, 23: 1, 155 — 172
To link to this Article: DOI: 10.1080/00958979109408248
URL: http://dx.doi.org/10.1080/00958979109408248

J. Coord. Chem. 1991, Vol. 23. pp. 155–172
Reprints available directly from the publisher
Photocopying permitted by license only

STRUCTURAL ASPECTS OF THE DEPHOSPHORYLATION OF ADENOSINE TRIPHOSPHATE CATALYZED BY POLYAMMONIUM MACROCYCLES

LIGANG QIAN, ZHONG SUN, JINNIAN GAO, BARAHMAN MOVASSAGH, LUIS MORALES, and KRISTIN BOWMAN MERTES*

Departments of Chemistry and Medicinal Chemistry, University of Kansas, Lawrence, Kansas 66045, U.S.A.

(Received July 6, 1990)

Four polyammonium macrocycles were synthesized and characterized: two with 21-membered rings and differing numbers of oxygen and nitrogen heteroatoms, [21]N_6O (**1**) and [21]N_5O_2 (**2**), and two with bipyridine incorporated into the ring, [24]N_4O_2bipy (**3**) and [27]N_5O_2bipy (**4**). Their ability to catalyze the dephosphorylation of adenosine triphosphate was examined. It was found that ring size plays a crucial role in the catalytic ability of the macrocycles, with the 21-membered rings being superior to larger macrocycles. Also, rates of dephosphorylation were found to increase with increasing number of nitrogen atoms in the ring. For two of the macrocycles, crystal structures were determined. Macrocycle **2** crystallizes in the triclinic space group $P\bar{1}$, $a = 10.692(1)$, $b = 17.037(2)$, $c = 8.1952(8)$ Å, $\alpha = 92.550(9)$, $\beta = 100.816(9)$, $\gamma = 106.77(1)°$, $V = 1396.1(3)$ Å^3; the structure was solved to $R = 0.089$ and $R_w = 0.098$. Macrocycle **4** crystallizes in the monoclinic space group $P2_1/n$, $a = 14.589(1)$, $b = 15.427(1)$, $c = 16.382(1)$ Å, $b = 90.137(6)°$, $V = 3687.0(9)$ Å^3; the structure was solved to $R = 0.056$ and $R_w = 0.085$.

Keywords: Polyammonium macrocycle, adenosine triphosphate, hydrolysis

INTRODUCTION

Simple polyammonium macrocycles have been found to be successful biomimics with respect to catalysis of phosphoryl transfer reactions.[1–6] These molecules are capable of forming high affinity complexes with a variety of anionic substrates, including nucleotides, through both electrostatic and hydrogen bonding interactions. In the case of nucleotides, complexation is followed by dephosphorylation, *i.e.*, cleavage of the terminal phosphate for di- and triphosphates, in some cases with an observed covalent macrocyclic phosphoramidate intermediate (Scheme 1).[1,2] While there are a number of potential macrocyclic catalysts for these reactions, large rate accelerations for dephosphorylation are noted only for a limited number of rings and appear to be related to size (between 21 and 24 atoms). For both larger and smaller rings rates are markedly slower. Furthermore, a recent thermodynamic study of simple macrocyclic polyamines has indicated that stability constants of macrocycle-nucleotide complexes ranging in size from 18 to 36 ring atoms and 6 to 12 amine nitrogens increase with decreasing size and increasing protonation of the ring.[7] Nonetheless, even when protonated, the 18-membered ring [18]N_6 is not nearly as good a catalyst as the 21- and 24-membered [21]N_7 and [24]N_8 analogues.[7] These findings agree with earlier

* Author for correspondence.

studies of the 18- and 24-membered ring macrocycles.[1] In fact, it was demonstrated in early studies that there is no direct correlation between the K_s for macrocycle–nucleotide complex formation and catalytic activity.[1]

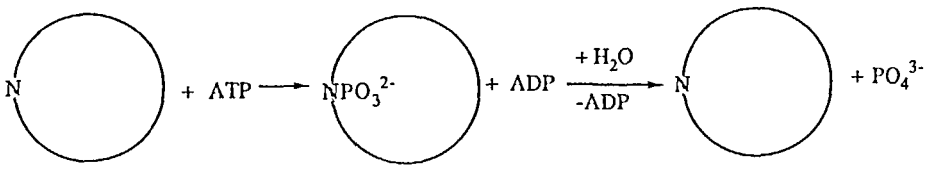

SCHEME 1

While quite a few studies have been made of the catalytic ability of a number of macrocycles of varying sizes and with a variety of pendant groups,[1–6] the simple macrocycles within a close size range (21 to 24 ring atoms) seem to be the best catalysts for the dephosphorylation of nucleotides. In order to probe some of the specific structural effects with respect to ring size, involved in this phosphoryl transfer catalysis, a series of closely related macrocycles, **1–4**, were synthesized. Two of these contain a bipyridine ring in order to investigate the effect of introducing the potential for interaction with the base portion of the nucleotide. The crystal structures have been determined for two of the new macrocycles. This information, along with crystal structure data for two of the most efficient macrocycles previously examined, $[21]N_7$[7] and $[24]N_6O_2$[8] (**5** and **6**, respectively), now allows for a better assessment of the structural requirements for catalysis.

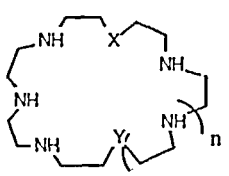

1 n = 1, X = O, Y = NH
2 n = 1, X = Y = O
5 n = 1, X = Y = NH
6 n = 2, X = Y = O

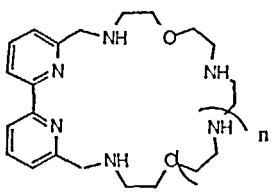

3 n = 1
4 n = 2

EXPERIMENTAL SECTION

Materials

N,N'-bis(*p*-tolylsulfonyl)ethylenediamine (**7**),[9] *N,N',N''*-tris(*p*-tolylsulfonyl)diethylenetriamine (**8**),[10] 7,10-bis(*p*-tolylsulfonyl)-1,16-bis(mesyloxy)-7,10-diaza-4,13-dioxadecane (**9**),[11] *N*-(*p*-tolylsulfonyl)aminoethoxyethanol (**10**),[12] and 6,6'-bis(chloromethyl)-2,2'-bipyridine (**11**),[13] were prepared as previously described.

1,4,7,10,13,16-Hexakis(diethylphosphoryl)-1,4,7,10,13,16-hexaazahexadecane (13)

To a solution containing pentaethylenehexamine (**12**) (5.00 g, 21.6 mmol) and triethylamine (15.7 g, 155 mmol) in 100 cm^3 CH_2Cl_2 was added dropwise a solution of

diethyl chlorophosphate (22.3 g, 129 mmol) in 50 cm^3 CH_2Cl_2 during 30 min under argon with stirring at 0°C. After the addition, the reaction mixture was stirred at room temperature for 48 h, washed with H_2O (3 × 60 cm^3), 1 M HCl (3 × 60 cm^3), 5% $NaHCO_3$ (3 × 60 cm^3), H_2O (3 × 60 cm^3) and dried over anhydrous Na_2SO_4. The solution was filtered and evaporated to dryness to give a yellow residue. Chromatography (SiO_2, 100:10 CH_2Cl_2–CH_3OH) gave the desired compound as an oil [4.33 g (19.1%)]. ^1H NMR ($CDCl_3$) 3.88–4.06 (26H, m, $POCH_2CH_3$ and PN*H*), 2.94–3.14 (20H, CH_2N), 1.25 (36H, t, J = 7 Hz, $POCH_2CH_3$) ppm; ^{13}C NMR ($CDCl_3$) 62.78, 62.70, 62.44, 62,36, 62.27, 62.08, 62.01, 47.20, 47.56, 45.74, 45.32, 40.16, 16.13, 16.05, 15.99, 15.96; HRMS (POS FAB) m/e for $C_{34}H_{83}N_6O_{18}P_6$ + 1H requires 1049.419, found 1049.421.

1,5-Bis(mesyloxy)-3-oxapentane (14)

To a mixture of diethylene glycol (8.00 g, 75.5 mmol) and triethylamine (33.5 g, 332 mmol) in CH_2Cl_2 (100 cm^3) under argon was added dropwise a solution of methanesulfonyl chloride (19.0 g, 166 mmol) in CH_2Cl_2 (30 cm^3) over a period of 30 min with stirring in an ice-NaCl bath. The reaction mixture was stirred at room temperature for 5 h, washed with H_2O (3 × 50 cm^3), 1m HCl (3 × 60 cm^3), 2% $NaHCO_3$ (3 × 60 cm^3), H_2O (3 × 60 cm^3), and dried over anhydrous Na_2SO_4. The solution was filtered and the solvent was evaporated to give a red oil. Crystallization from CH_3CH_2OH gave the white crystalline product [13.3 g (67.2%)], m.p. 55–56.5°C (lit. 57–58°C).[14] ^1H NMR ($CDCl_3$) 4.35 (4H, t, J = 6 Hz, $MsOCH_2$), 3.77 (4H, t, J = 6 Hz, CH_2O), 3.04 (6H, s, SO_2CH_3) ppm; ^{13}C NMR ($CDCl_3$) 68.90, 68.78, 37.51 ppm; MS (CI–NH_3) m/e 263 (M + 1).

4,7,10,13,16,19-Hexakis(diethylphosphoryl)-1-oxa-4,7,10,13,16,19-hexaazacycloheneicosane (15)

To a suspension of NaH (82 mg, 3.43 mmol) in 100 cm^3 DMSO under argon was added the solution of **14** (1.50 g, 1.43 mmol) in 30 cm^3 DMSO with stirring. The mixture was heated in an oil bath at 60°C until no more gas was released, then cooled in an ice bath. The solution of **13** (374 mg, 1.43 mmol) in 20 cm^3 DMSO was added and the mixture was stirred at 80°C for 48 h. The DMSO was evaporated and the residue was dissolved in 100 cm^3 CH_2Cl_2, washed with H_2O (3 × 50 cm^3) and dried over anhydrous Na_2SO_4. After filtration, the solvent was evaporated to dryness, and the residue was chromatographed (SiO_2, 100:10 CH_2Cl_2–CH_3OH) to give the light yellow oil product [817 mg (51.1%)]. ^1H NMR ($CDCl_3$) 3.92 (24H, q, J = 6.9, $POCH_2CH_3$), 3.46 (4H, t, J = 5.4 Hz, CH_2O), 2.89–3.08 (24H, m, NCH_2), 1.21 (36H, t, J = 6.9 Hz, $POCH_2CH_3$) ppm; ^{13}C NMR ($CDCl_3$) 71.20, 62.17, 62.09, 62.00, 61.92, 46.46, 46.41, 46.10, 45.98, 45.93, 45.55, 45.36, 16.01, 15.92 ppm; HRMS (POS FAB) m/e for $C_{38}H_{89}N_6O_{19}P_6$ + 1H requires 1119.461, found 1119.462.

1-Oxa-3,7,10,13,16,19-hexaazacycloheneicosane (1)

The protected macrocycle **15** (800 mg, 0.716 mmol) was dissolved in CH_2Cl_2 (3 cm^3) and CH_3OH (12 cm^3) was added to obtain a clear solution, which was cooled in an ice bath and saturated with HCl gas. The solution was allowed to remain at room temperature for 70 h; ether was added, and the resulting precipitate was filtered and

washed with ether. The product was passed through an anion exchange resin column (Dowex-1-OH) eluting with H_2O to obtain the free amine as a semisolid [175 mg (80.9%)]. ^1H NMR ($CDCl_3$) 3.51 (4H, t, J = 5.0 Hz, CH_2O), 2.66–2.76 (24H, m, CH_2N), 1.78 (6H, s, b, N*H*) ppm; ^{13}C NMR ($CDCl_3$) 70.48, 49.35, 49.28 ppm; HRMS (POS FAB) m/e for $C_{14}H_{35}N_6O$ + 1H requires 303.287, found 303.288.

*4,7,10,16,19-Pentakis(*p*-tolylsulfonyl)-1,13-dioxa-4,7,10,16,19-pentaazacyclohene-icosane (16)*

A mixture of the triamine **8** (5.65 g, 10 mmol) and Cs_2CO_3 (16.3 g, 0.05 mol) in DMSO (150 cm^3) was heated at 80°C for 0.5 h. To this solution was added a solution of **9** (8.52 g, 10 mmol) in DMSO (150 cm^3), and the mixture was stirred overnight at 80°C. The solution was concentrated *in vacuo*, diluted with CH_2Cl_2 (200 cm^3), washed with H_2O (200 cm^3) and saturated NaCl (100 cm^3), and dried over anhydrous $MgSO_4$. The residue, after evaporation, was purified by column chromatography (SiO_2, 100:2 CH_2Cl_2:CH_3OH) to give the pure product as a foam [8.0 g (74%)]. ^1H NMR ($CDCl_3$) 7.73–7.64 (10H, m, aromatic), 7.32 (10H, d, J = 7.8 Hz, aromatic), 3.60 (8H, br, s, (CH_2O), 3.39 (8H, br, s, CH_2N), 3.37 (4H, s, CH_2N), 3.33, 3.22 (4H each, t, J = 4.0 Hz, CH_2N), 2.44 (15H, s, ArCH_3) ppm. ^{13}C NMR 142.73, 142.54, 142.36, 134.85, 134.09, 133.50, 128.76, 128.71, 126.39, 126.33, 126.20, 69.70, 68.87, 49.10, 48.86, 48.79, 20.45 ppm. Anal.: Calcd. for $C_{49}H_{63}N_5O_{12}S_5$: C, 54.78; H, 5.91; N, 6.52%. Found: C, 54.38; H, 5.99; N, 6.99%.

*6,6'-Bis(*N*-(2-(2-hydroxyethoxy)ethyltosylamidomethyl)-2,2'-bipyridine (17)*

A solution of *N*-tosylaminoethyoxyethanol (**10**) (7.8 g, 0.03 mol) in DMF (50 cm^3) was added dropwise to a suspension of NaH (0.72 g, 0.03 mol) in DMF (50 cm^3) with stirring in an ice bath. After the addition was complete, the solution was heated to 70°C and a solution of the substituted bipyridine (**11**) (2.25 g, 0.01 mol) in DMF (50 cm^3) was added over a period of 1 h. The mixture was then stirred for an additional 3 h. The DMF was removed *in vacuo*, and the residue was diluted with CH_2Cl_2 (100 cm^3) and washed with water and saturated NaCl solution (100 cm^3 each). The organic layer was dried over K_2CO_3 and concentrated *in vacuo*. The residue was chromatographed (SiO_2, 100:2 CH_2Cl_2–CH_3OH) to give a white solid, which was recrystallized from CH_2Cl_2-toluene [4.5 g (64%)]: mp 116.5–117.5°C. ^1H NMR ($CDCl_3$) 8.09 (2H, d, J = 7.8 Hz, py), 7.77 (2H, t, J = 7.5 Hz, aromatic), 7.51 (2H, d, J = 7.8 Hz, py), 7.28 (4H, d, aromatic), 4.64 (4H, s, pyCH_2), 3.50 (8H, s, CH_2O), 3.47 (4H, t, J = 4.0 Hz, CH_2OMs), 3.30 (4H, t, J = 4.0 Hz, CH_2N), 2.60 (2H, br, s, O*H*), 2.39 (6H, s, ArCH_3) ppm; ^{13}C NMR 156.61, 155.02, 143.41, 137.59, 136.68, 129.66, 122.31, 119.78, 72.16, 69.26, 61.31, 54.05, 48.07, 21.43 ppm. EIMS m/e (rel. intens.) 699 (M^+ + 1, 10) 543 (M^+ − Ts, 50), 467 (30). Anal.: Calcd. for $C_{34}H_{42}N_4O_8S_2$: C, 58.43, H, 6.06, N, 8.02%. Found: C, 58.64; H, 6.00; N, 7.89%.

*6,6'-Bis(*N*-(2-(2-mesyloxyethoxy)ethyltosylamidomethyl)2,2'-bipyridine (18)*

A mixture of the diol **17** (0.7 g, 1 mmol) and triethylamine (0.5 g, 4.76 mmol) in CH_2Cl_2 (20 cm^3) was cooled in a dry ice–isopropyl alcohol bath. To this solution was added a solution of mesyl chloride (0.24 g, 2.1 mmol) in CH_2Cl_2 (5 cm^3). The mixture was allowed to warm up to room temperature, stirred for an additional 4 h, and washed with 1 M HCl (100 cm^3), saturated $NaHCO_3$ (20 cm^3), and saturated

NaCl (20 cm^3). The organic layer was dried over Na_2SO_4 and concentrated *in vacuo*. The residue was recrystallized from CH_2Cl_2–ether to give pure product [0.81 g (94%)]: mp 132–133°C. ^1H NMR ($CDCl_3$) 8.09 (2H, d, J = 7.8 Hz, py), 7.76 (2H, t, py), 7.71 (4H, d, J = 8.5 Hz, aromatic), 7.47 (2H, d, py), 7.26 (4H, d, aromatic), 4.61 (4H, s, pyCH_2), 4.18 (4H, m, CH_2O), 3.56–3.49 (12H, m, CH_2N, CH_2O), 2.97 (6H, s, OSO_2CH_3), 2.38 (6H, s, ArCH_3) ppm; ^{13}C NMR 156.48, 155.06, 143.48, 137.58, 136.65, 129.71, 127.23, 122.49, 119.64, 69.65, 68.75, 68.55, 54.56, 48.33, 37.57, 21.50 ppm. Anal.: Calcd. for $C_{36}H_{46}N_4O_{12}S_4$: C, 50.57; H, 5.42; N, 6.55%. Found: C, 50.18, H, 5.40; N, 6.19%.

*8,14,17,23-Tetrakis(*p*-tolylsulfonyl)-8,14,17,23,29,30-hexaaza-11,20-dioxatricyclo-[24.3.1.$1^{2,6}$]triaconta-2,4,6,26,28,29-hexaene (19)*

To a suspension of NaH (73 mg, 60% in oil, freshly washed with hexane) in DMSO (10 cm^3) was added dropwise a solution of the diamine **7** (302 mg, 0.82 mmol) in DMSO (10 cm^3) over a period of 0.5 h at room temperature. After bubbling ceased, the dimesylate **18** (700 mg, 0.82 mmol) in DMSO (30 cm^3) was added. The mixture then was heated to 80°C and stirred for 10 h. Concentration and chromatography (SiO_2, 100:2 CH_2Cl_2 : CH_3OH) gave the product as a foam [405 mg (48%)]. ^1H NMR ($CDCl_3$) 8.11 (2H), d, J = 7.8 Hz, py), 7.74 (4H, d, J = 8.4 Hz, aromatic), 7.73 (2H, t, py), 7.52, 7.51 (6H, d each, py and aromatic), 7.33, 7.25 (4H each, d, aromatic), 4.49 (4H, s, pyCH_2), 3.39, 3.33 (4H each, t, J = 5.4 Hz, CH_2O), 3.14, 2.83, 2.81 (4H each, CH_2N), 2.43, 2.40 (6H each, s, ArCH_3) ppm; ^{13}C NMR 156.94, 154.74, 143.64, 143.48, 137.75, 136.15, 135.72, 129.90, 129.71, 127.20, 127.08, 122.70, 119.66, 69.82, 69.18, 55.27, 49.03, 48.99, 48.42, 21.56, 21.52 ppm. EIMS m/e (rel. intens.) 875 (M^+ – Ts, 20), 719 (M^+ – 2Ts, 30), 648 (10). Anal.: Calcd. for $C_{50}H_{50}N_6O_{10}S_4$: C, 58.23; H, 5.67; N, 8.13%. Found: C, 57.88;, H, 5.77; N, 7.90%.

*8,14,17,20,26-Pentakis(*p*-tolylsulfonyl)-8,14,17,20,26,32,33-heptaaza-11,23-dioxatricyclo[27.3.1.$1^{2,6}$]tritriaconta-2,4,6,29,31,32-hexaene (20)*

A mixture of the triamine **8** (113 mg, 0.2 mmol) and Cs_2CO_3 (0.65 g, 2 mmol) in DMF (20 cm^3) was heated to 80°C, stirred for 0.5 h, and cooled to 0°C. Into this solution was poured a solution of the dimesylate **16** (170.8 mg, 0.2 mmol) in DMF (20 cm^3). The mixture was stirred at 80°C for 20 h and concentrated *in vacuo*. The residue was diluted with CH_2Cl_2 (20 cm^3) and washed with water (20 cm^3). The organic layer was dried over anhydrous Na_2SO_4. Concentration and chromatography (SiO_2, 100:1 $CH_2Cl_2CH_3OH$) gave **3** as a foam [150 mg (61%)]. ^1H NMR ($CDCl_3$ 7.98 (2H, m, py), 7.68–7.40 (10H, m, aromatic and py), 7.24 (6H, m, aromatic), 4.55, 453 (2H each, pyCH_2), 3.42–3.27, 3.00–2.92 (24H, m, CH_2N and CH_2O), 2.38, 2.36, 2.35 (3H each, s, ArCH_3) ppm. ^{13}C NMR 156.56, 154.83, 143.49, 137.52, 136.40,. 135.92, 135.56, 129.76, 127.17, 122.55, 119.60, 70.09, 69.49, 54.91, 49.03, 48.50, 48.27, 48.22, 21.52 ppm. Anal.: Calcd. for $C_{59}H_{69}N_7O_{12}S_5$: C, 57.68; H, 5.66; N, 7.98%. Found: C, 57.29, H, 5.82; N, 7.68%.

Generalized Detosylation Procedure

The tosylated macrocycle (1 mmol) and phenol (10–15 mmol) were dissolved in 32% HBr in acetic acid (10–15 cm^3). The mixture was heated to 80°C and stirred for 72 h. After cooling to room temperature, ether (50 cm) was added to precipitate the salt,

which was collected by filtration and rinsed with ether. The salt was dissolved in H_2O (2 cm^3) and passed through an anion exchange resin (Dowex-1, HO-form) to obtain the free amine after removal of solvent.

*1,13-Dioxa-4,7,10,16,19-pentaazacycloheneicosane (**2**):* [285 mg (94%)] as a semi-solid. ^1H NMR (D_2O) 3.58 (8H, t, J = 4.2 Hz, CH_2O), 2.75 (8H, t, CH_2N), 2.71 (12H, br, s, CH_2N) ppm. ^{13}C NMR (H_2O) 72.16, 72.02, 50.80, 50.50, 50.42, 50.10 ppm. EIMS m/e (rel. intens.) 304 ($M^+ + 1$, 18), 259(30), 247(25), 235(24), 204(15). HRMS: Calcd. for $C_{14}H_{33}N_5O_2$ + 1H: 304.2712. Found: 304.2716. Anal.: Calcd. for $C_{14}H_{33}N_5O_2 \cdot 5HBr \cdot CH_3OH$: C, 24.35; H, 5.72; N, 9.46%. Found: C, 24.10; H, 5.40; N, 9.30%. Crystals of the HBr salt suitable for X-ray analysis were obtained from methanol.

*8,14,17,23,29,30-Hexaaza-11,20-dioxatricyclo[24.3.1.$1^{2,6}$]triaconta-2,4,6,26,28,29-hexaene (**3**):* [335 mg (81%)] as an oil. ^1H NMR (D_2O) 7.76–7.67 (4H, m, py) 7.30 (2H, d, J = 6.9 Hz, py), 3.77 (4H, s, pyCH_2), 3.47, 3.35 (4H, each, br, s, CH_2O), 2.66, 2.49 (4H each, br, s, CH_2N), 2.34 (4H, s, CH_2N) ppm; ^{13}C NMR 161.67, 157.89, 141.27, 126.41, 123.66, 71.86, 71.28, 55.75, 50.01, 49.76, 49.65 ppm. EIMS m/e (rel. intens.) 415 ($M^+ + 1H$, 30), 358(25), 298(30), 244(75). HRMS: Calcd. for $C_{22}H_{34}N_6O_2$: 414.2743; Found: 414.2747. Anal.: Calcd. for $C_{22}H_{34}N_6O_2 \cdot 5HBr$: C, 32.26; H, 4.80; N, 10.26%. Found: C, 32.20; H, 5.18; N, 9.88%.

*8,14,17,20,26,32,33-Heptaaza-11,23-dioxatricyclo[27.3.1.$1^{2,6}$]tritriaconta-2,4,6,29,31,32-hexaene (**4**):* [366 mg (80%)] as an oil. ^1H NMR ($CDCl_3$) 8.35 (2H, d, J = 7.8 Hz, py), 7.83 (2H, t, py), 7.36 (2H, d, J = 7.3 Hz, py), 4.03 (4H, s, pyCH_2), 3.67 (4H, t, J = 4.0 Hz, CH_2O), 3.59 (4H, t, J = 4.3 Hz, CH_2O), 2.93, 2.76, 2.55, 2.50 (4H each, t, CH_2N), 2.33 (5H, br, s, N*H*) ppm. ^{13}C NMR 159.06, 155.62, 137.18, 122.20, 119.28, 69.93, 69.87, 54.60, 49.24, 49.15, 49.06, 48.74 ppm. EIMS m/e (rel. intens.) 476 ($M^+ + 1$, 20), 475 (M^+, 19), 401(30), 298(30). HRMS: Calcd. for $C_{24}H_3C_9N_7O_2$: 457.3165. Found: 457.3160. Anal.: Calcd. for $C_{24}H_{39}N_7O_2 \cdot 6HCl \cdot 2.5H_2O$: 39.96; H, 6.99; N, 13.59%. Found: C, 40.09; H, 7.09; N, 13.68%. Crystals suitable for X-ray analysis were obtained by recrystallization from methanol.

Methods

NMR spectra were recorded on a Varian XL-300 Spectrometer at 300 MHz for ^1H, 75.43 MHz for ^{13}C, and 122 MHz for ^{31}P. Chemical shifts (ppm) are relative (+, downfield) to references of tetramethylsilane or sodium 3-(trimethylsilyl)propanesulfonate. The probe temperature was regulated by a variable temperature accessory. The use of low decoupler power for heteronuclear decoupling at the reported concentrations of reagents and salts in 5-mm NMR tubes did not result in apparent temperature variations.

Mass spectra were obtained from Ribermag R-10-10 and VG-ZAB spectrometers. Microanalyses were performed on a Hewlett-Packard 185 microanalytical instrument. The solution pH was recorded at 22 or 25°C with a Radiometer pH meter.

HPLC Kinetic Analysis

A Waters Model 501 high-performance liquid chromatograph with a Waters Model

481 absorbance detector and Model 740 data analyzer was used. Samples were injected on a silica column containing amine groups (Waters Bondpak-NH_2). The mobile phase was a mixture of 15% acetonitrile and 85% 0.05 M ammonium phosphate at pH 4.5. Aqueous solutions (in 20 μL aliquots) of ATP and macrocycle were quenched by addition to 40 μL of the mobile phase adjusted to pH 10.5 prior to injection. Resolution of AMP, ADP, and ATP afforded integral values used in the determination of the concentrations of the species at each time point.

NMR Kinetic Analyses

Kinetic studies were performed by following the time-dependent change in integrals from the ^{31}P NMR signals of the substrate and products phosphorus atoms. By this method, the calculated standard deviation for the observed rates was 6%. A 0.5 cm^3 solution containing 0.02 M ATP and the macrocycle as its hexahydrohalide salt (0.02 M) in 10% D_2O/H_2O was placed in the NMR probe in a 5 mm tube at the desired temperature. An automated program ensured an adequate number of acquisitions were accumulated for each sequential spectrum over a period of several half-lives.

TABLE I
Crystallographic data for [21]N_5O_2 (2) and [27]N_5O_2bipy (4).

compound	$C_{15}H_{38}N_5O_3Br_5$	$C_{26}H_{51}N_7O_4Cl_6$
fw	736.02	738.45
a, Å	10.692(1)	14.589(1)
b, Å	17.037(2)	15.427(1)
c, Å	8.1952(8)	16.382(1)
α, deg	92.550(9)	
β, deg	100.816(9)	90.137(6)
γ, deg	106.77(1)	
V, Å^3	1396.1(3)	3687.0(9)
ρ_{calcd}, g cm^{-3}	1.751	1.330
Z	2	4
space group	$P\bar{1}$	$P2_1/n$
cryst. dimens., mm	0.40 × 0.40 × 0.50	0.10 × 0.30 × 0.50
temp., °C	23	23
radiatn.	CuK_α	CuK_α
diffractometer	Rigaku AFC5R	Rigaku AFC5R
μ, cm^{-1}	90.10	46.79
no. indep. reflecns	3863	5314
no. with $I > 3\sigma(I)$	3279	3921
no. variables	291	568
reflecn./parameter	11.27	6.90
final R*	0.089	0.056
final R_w*	0.098	0.085

*$R = \sum||F_o| - |F_c||/\sum|F_o|$ and $R_w = [(\sum w(|F_o| - |F_c|)^2/\sum wF_o^2]^{1/2}$.

Crystal Structure Data Collection and Reduction

Crystal structure data are provided in Table I. All measurements were made on a Rigaku AFC5R diffractometer with graphite monochromated CuK_α radiation and a

12 KW rotating anode generator. Cell constants and an orientation matrix for data collection were obtained from a least-squares refinement using the setting angles of 25 carefully centred reflections. The data were collected at a temperature of 23 ± 1°C using the ω-2θ scan technique to a maximum 2θ value of 112.1°. Weak reflections ($I < 10.0\sigma(I)$) were rescanned (maximum 2 rescans), and the counts were accumulated to ensure good counting statistics. Stationary background counts were recorded on each side of the reflection. The ratio of peak to background counting times was 2 : 1. The diameter of the incident beam collimator was 0.5 mm and the crystal to detector distance was 285.0 nm.

The intensities of three representative reflections were measured after every 150 reflections. For [21]N_5O_2, these remained essentially constant, but for [27]N_5O_2bipy they decayed by 7.9%, so a linear correction factor was applied to the data. An empirical absorption correction, based on azimuthal scans of several reflections, was applied.[15] The data were corrected for Lorentz and polarization effects. No extinction corrections were applied.

Crystal Structure Solution and Refinement

The structures were solved by direct methods.[16] Refinement was performed using full-matrix least-squares methods. The non-hydrogen atoms were refined anisotropically. Hydrogen atom positions were located from a difference map after all the nonhydrogens were located. The weighting scheme was based on counting statistics and included a factor ($p = 0.05$) to downweight the intense reflections. Neutral atom scattering factors were taken from Cromer and Waber.[17] Anomalous dispersion effects were included in F_{calc}.[18] All calculations were performed using the TEXSAN[15] crystallographic software package of the Molecular Structure Corporation. While the final R values are relatively high, this is not unusual for macrocylic structures of this size, since these molecules are difficult to crystallize and often retain solvent molecules of crystallization which are disordered. The final atomic coordinates and isotropic thermal parameters for non-hydrogen atoms are listed in Table II.

RESULTS AND DISCUSSION

Synthesis

The synthetic pathways for macrocycles **1** through **4** are shown in Schemes 2–4. Several modifications have been made to previously established routes for macrocyclic synthesis, and have resulted in improved yields.

The route to [21]N_6O (Scheme 2) employed the use of diethyl phosphoryl protecting groups for the macrocyclic amines. Initially the common tosylate protection was used, with subsequent deprotection using 30% HBr/acetic acid at 80°C, as for the other three macrocycles. These efforts gave an impure product, despite pure starting material, which was extremely difficult to purify. Attempts at detosylation using LAH in refluxing THF as well as concentrated H_2SO_4 at 100°C also resulted in a mixture of complex products. By using the diethyl phosphoryl protecting group, much milder deprotection procedures (HCl gas, 0°C, in a CH_2Cl_2/CH_2OH mixture) could be used, which led to the pure product. The analogous 21-membered [21]N_5O_2 was, on the other hand, readily accessible by the established tosylate procedure (Scheme 3).

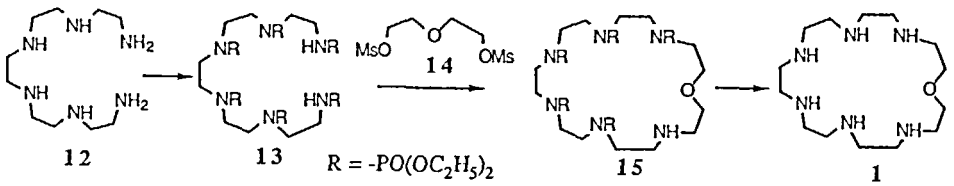

SCHEME 2

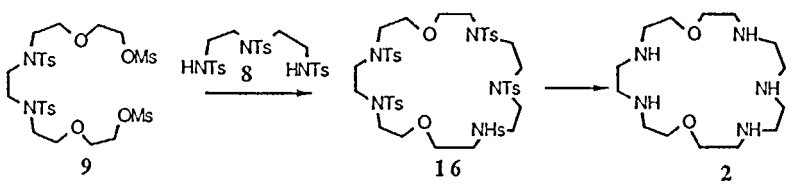

SCHEME 3

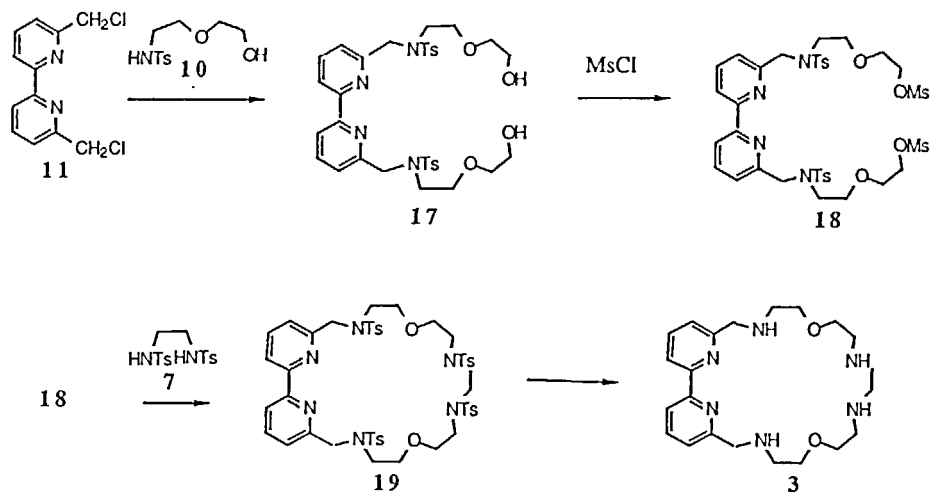

SCHEME 4

Macrocycles similar to the [24]N_4O_2bipy and [27]N_5O_2bipy have been reported by this group.[12] Modifications have been made to the previously published procedure, however, which result in a greater overall yield of the macrocycle (Scheme 4). The 6,6′-bis-(*N*-tosylamidomethyl)-2,2′-bipyridine precursor to the macrocycle can be achieved in 29% yield, and reacted with the mesylated "eastern" half diamine **9** or its triamine analogue. This actually gives fairly high yields for **3** and **4** (76% and 57%, respectively). Nonetheless, the overall yield in two steps from the starting 6,6′-dimethyl-2,2′-pyridine is approximately 5%. Hence, the route shown in Scheme 4 was used, and resulted in a yield of **17** of 64%.

TABLE II
Positional and isotropic thermal parameters with esd's for [21]N_5O_2 (2) and [27]N_5O_2bipy (4).

atom	*x/a*	*y/b*	*z/c*	*B*(eq)
		[21]N_5O_2 (2)		
Br(1)	0.4870(1)	0.18401(8)	0.0775(2)	3.04(5)
Br(2)	0.7767(1)	0.09995(9)	0.8661(2)	3.88(6)
Br(3)	0.4268(1)	0.35082(9)	0.7921(2)	3.48(6)
Br(4)	0.0769(2)	0.1547(1)	0.4641(2)	4.50(7)
Br(5)	0.1667(2)	0.4663(1)	0.1341(3)	5.18(8)
O(1)	0.591(1)	0.3828(6)	1.301(1)	3.8(3)
C(2)	0.502(2)	0.4164(9)	1.368(2)	4.2(5)
C(3)	0.371(2)	0.351(1)	1.340(2)	3.9(5)
N(4)	0.316(1)	0.3278(7)	1.159(1)	3.3(4)
C(5)	0.186(1)	0.2614(8)	1.117(2)	3.6(5)
C(6)	0.132(1)	0.2370(9)	0.934(2)	3.6(5)
N(7)	0.186(1)	0.1764(6)	0.863(1)	2.9(4)
C(8)	0.131(1)	0.0913(8)	0.911(2)	3.4(5)
C(9)	0.152(1)	0.0249(9)	0.801(2)	3.8(5)
O(10)	0.285(1)	0.0129(6)	0.846(1)	4.8(4)
C(11)	0.316(2)	−0.0356(8)	0.712(2)	4.0(5)
C(12)	0.336(2)	0.011(1)	0.564(2)	4.2(5)
N(13)	0.438(1)	0.0852(6)	0.622(1)	2.8(3)
C(14)	0.447(1)	0.146(1)	0.505(2)	3.9(5)
C(15)	0.586(2)	0.206(1)	0.554(2)	3.9(5)
N(16)	0.618(1)	0.2352(6)	0.733(1)	2.9(4)
C(17)	0.749(2)	0.3030(9)	0.779(2)	4.1(5)
C(18)	0.801(1)	0.3216(9)	0.964(2)	3.8(5)
N(19)	0.729(1)	0.3698(7)	1.048(1)	3.1(4)
C(20)	0.797(2)	0.400(1)	1.221(2)	4.6(6)
C(21)	0.718(2)	0.442(1)	1.306(2)	4.6(6)
O(1S)	0.931(1)	0.2942(9)	0.511(2)	7.3(6)
C(1S)	1.040(2)	0.369(1)	0.561(3)	6.9(8)
		[27]N_7O_2 bipy (4)		
Cl(1)	0.4022(1)	0.18695(8)	0.38570(8)	4.07(6)
Cl(2)	0.5707(1)	0.35362(8)	0.5072(1)	4.26(7)
Cl(3)	0.9981(1)	0.0664(1)	0.61391(9)	5.06(7)
Cl(4)	0.2204(1)	0.3238(1)	0.60992(9)	4.63(7)
Cl(5)	0.7063(1)	0.4094(1)	0.7731(1)	4.93(7)
Cl(6)	0.0168(1)	0.4262(1)	0.3710(1)	4.55(7)
O(1S)	0.7499(4)	0.2040(3)	0.7830(3)	7.1(3)
O(2S)	0.2295(7)	0.2488(8)	0.7856(5)	7.3(6)
O(15)	0.4512(2)	0.3461(2)	0.8617(2)	3.6(2)
O(27)	0.8891(2)	0.3695(2)	0.5779(2)	3.9(2)
N(12)	0.6124(3)	0.3852(3)	0.9594(3)	3.3(2)
N(18)	0.5050(3)	0.4437(3)	0.7311(3)	3.3(2)
N(21)	0.5978(3)	0.6195(3)	0.5997(3)	3.8(2)
N(24)	0.8197(3)	0.5275(3)	0.5175(3)	3.6(2)
N(30)	0.9799(3)	0.4044(3)	0.7303(3)	3.4(2)
N(32)	0.9746(3)	0.5091(3)	0.8649(2)	3.1(2)
N(33)	0.8268(3)	0.4921(3)	0.9558(3)	2.9(2)
C(1)	1.0514(3)	0.5089(3)	0.8218(3)	3.4(2)

TABLE II (*continued*)

[21]N_5O_2 (2)				
atom	*x/a*	*y/b*	*z/c*	*B*(eq)
C(1S)	0.6986(6)	0.1691(5)	0.7165(4)	6.9(4)
C(2)	1.1150(4)	0.5764(4)	0.8265(3)	3.9(3)
C(2S)	0.1781(8)	0.1802(8)	0.7908(7)	4.3(5)
C(3)	1.0968(4)	0.6452(4)	0.8779(4)	4.1(3)
C(4)	1.0165(3)	0.6455(4)	0.9245(3)	3.4(2)
C(5)	0.9585(3)	0.5759(3)	0.9154(3)	3.0(2)
C(6)	0.8726(3)	0.5680(3)	0.9628(3)	2.9(2)
C(7)	0.8369(4)	0.6321(4)	1.0121(3)	3.6(3)
C(8)	0.7559(4)	0.6165(4)	1.0524(4)	4.2(3)
C(9)	0.7110(4)	0.5375(4)	1.0430(4)	3.8(3)
C(10)	0.7482(3)	0.4751(3)	0.9947(3)	3.0(2)
C(11)	0.7090(4)	0.3858(4)	0.9847(5)	3.8(3)
C(13)	0.5765(4)	0.2955(4)	0.9458(4)	3.5(3)
C(14)	0.4766(4)	0.2958(4)	0.9308(3)	3.6(3)
C(16)	0.4640(5)	0.3023(4)	0.7863(4)	4.5(3)
C(17)	0.4429(5)	0.3682(4)	0.7193(4)	4.6(3)
C(19)	0.5023(4)	0.5057(4)	0.6631(3)	3.8(3)
C(20)	0.5714(5)	0.5776(4)	0.6784(3)	3.9(3)
C(22)	0.6598(4)	0.5691(4)	0.5454(4)	3.6(3)
C(23)	0.7542(4)	0.5566(4)	0.5812(4)	3.7(3)
C(25)	0.8007(4)	0.4414(4)	0.4795(4)	4.1(3)
C(26)	0.8018(4)	0.3702(4)	0.5399(4)	4.2(3)
C(28)	0.8980(4)	0.3057(4)	0.6399(4)	3.8(3)
C(29)	0.9859(4)	0.3220(4)	0.6839(3)	3.7(3)
C(31)	1.0658(4)	0.4303(4)	0.7693(4)	4.1(3)

Kinetics

The dephosphorylation of ATP as catalyzed by **1–4** was followed by HPLC techniques, and, in some cases, by ^{31}P NMR (Table III).There is a definite correlation between ring size and hydrolytic efficiency. The 21-membered rings are exceptionally good catalysts. At lower pH's, however, neither the [21]N_6O, **1**, nor the [21]N_5O_2, **2**, can rival [21]N_7, **5**, for which the reaction is too fast to be followed at 70°C by either HPLC or NMR techniques.[7] For the 21-membered series, rates appear to increase with increasing number of nitrogen atoms in the ring. This is probably associated with the increasing charge density, which results in more successful complexation and subsequent electrostatic catalysis. Furthermore, there is a definite increase in rate in progressing from higher to lower pH for all of the ligands examined. This finding is as anticipated, since a greater degree of protonation exists at lower pH, which again facilitates complex formation.

The introduction of unsaturated groups into the ring greatly reduces the ability to catalyze ATP cleavage. This may be a reflection of different structural effects caused by the bipyridine rings, as discussed below, as well as increased steric hindrance. Previous studies in which pendant side chains were placed on [24]N_6O_2 (**6**) found that catalysis is extremely sensitive to steric hindrance, with rates diminishing when either one or two side chains are introduced.[4b]

TABLE III

First-order rate constants ($\times 10^3$, min^{-1}) for the dephosphorylation of a 1:1 molar ratio of ATP and macrocycles 1–4 (4×10^{-5} M) at 70°C.

macrocycle	pH 4	pH 7
[21]N_5O_2 (1)	132	9.90
[21]N_6O (2)	544	14.7
[24]N_4O_2bipy (3)	0.898	0.625
[27]N_5O_2bipy (4)	5.80	0.618

TABLE IV

Selected interatomic distances for [21]N_5O_2 (2) and [27]N_5O_2bipy (4).

atoms	distances, Å	atoms	distances, Å
		[21]N_5O_2	
O(1)–C(2)	1.41(2)	C(11)–C(12)	1.50(2)
O(1)–C(21)	1.43(2)	C(12)–N(13)	1.40(2)
C(2)–C(3)	1.49(2)	N(13)–C(14)	1.44(2)
C(3)–N(4)	1.48(2)	C(14)–C(15)	1.51(2)
N(4)–C(5)	1.49(2)	C(15)–C(16)	1.47(2)
C(5)–C(6)	1.49(2)	N(16)–C(17)	1.50(2)
C(6)–N(7)	1.47(2)	C(17)–C(18)	1.50(2)
N(7)–C(8)	1.50(2)	C(18)–N(19)	1.50(2)
C(8)–C(9)	1.50(2)	N(19)–C(20)	1.46(2)
C(9)–O(10)	1.48(2)	C(20)–C(21)	1.50(2)
O(10)–C(11)	1.48(2)	O(1S)–C(1S)	1.43(2)
		[27]N_5O_2]bipy	
C(1)–C(2)	1.397(8)	C(13)–C(14)	1.477(8)
C(1)–C(31)	1.501(8)	C(14)–O(15)	1.422(7)
C(2)–C(3)	1.381(8)	O(15)–C(16)	1.420(7)
C(3)–C(4)	1.400(8)	C(16)–C(17)	1.527(9)
C(4)–C(5)	1.375(7)	C(17)–N(18)	1.488(7)
C(5)–C(6)	1.482(7)	N(18)–C(19)	1.469(7)
C(6)–C(7)	1.380(7)	C(19)–C(20)	1.520(8)
C(7)–C(8)	1.376(8)	C(20)–N(21)	1.494(7)
C(8)–C(9)	1.392(9)	N(21)–C(22)	1.490(7)
C(9)–C(10)	1.359(8)	C(22)–C(23)	1.507(8)
C(10)–C(11)	1.501(8)	C(23)–N(24)	1.487(7)
C(11)–N(12)	1.469(7)	N(24)–C(25)	1.492(8)
N(12)–C(13)	1.496(7)	C(25)–C(26)	1.478(9)
C(28)–C(29)	1.491(8)	N(32)–C(1)	1.325(6)
C(26)–O(27)	1.416(7)	N(32)–C(5)	1.342(6)
O(27)–C(28)	1.419(7)	N(33)–C(6)	1.351(6)
N(30)–C(29)	1.485(7)	N(33)–C(10)	1.340(6)
N(30)–C(31)	1.461(8)	O(15)–C(15)	1.425(8)

The rates of dephosphorylation were followed by ^{31}P NMR for [21]N_5O_2 (2) and [27]N_5O_2bipy (4). In neither case was any evidence of macrocyclic phosphoramidate

(Scheme 1) observed. This does not necessarily mean that the reactions do not proceed *via* this mechanism, since phosphoramidates have been observed to be extremely unstable under the reaction conditions employed.[7] The rate of dephosphorylation of the bipyridine macrocycle **4** was extremely slow as anticipated. Resolution was poor, so an exact rate was not obtained. On the other hand at 70°C and pH 7.0, the first order rate constant for **2** was $0.050\,min^{-1}$ for a 1:1 ratio of 2:ATP (0.02 M in each). This rate can be compared to rates under similar conditions of $0.023\,min^{-1}$ for $[24]N_6O_2$, **6**,[4a] and $0.088\,min^{-1}$ for $[21]N_7$, **5**.[7] Again this indicates a crucial dependence on both ring size and charge density, with the [21]-membered macrocycle containing the largest number of nitrogen atoms being the most efficient.

TABLE V
Selected bond angles for $[21]N_5O_2$ (**2**) and $[27]N_5O_2$bipy (**4**).

atoms	angle, deg	atoms	angle, deg
		$[21]N_5O_2$	
C(2)-O(1)-C(21)	113(1)	C(11)-C(12)-N(13)	107(1)
O(1)-C(2)-C(3)	107(1)	C(12)-N(13)-C(14)	114(1)
C(2)-C(3)-N(4)	110(1)	N(13)-C(14)-C(15)	107(1)
C(3)-N(4)-C(5)	114(1)	C(14)-C(15)-N(16)	111(1)
N(4)-C(5)-C(6)	114(1)	C(15)-N(16)-C(17)	111(1)
C(5)-C(6)-N(7)	114(1)	N(16)-C(17)-C(18)	113(1)
C(6)-N(7)-C(8)	113(1)	C(17)-C(18)-N(19)	114(1)
N(7)-C(8)-C(9)	114(1)	C(18)-N(19)-C(20)	112(1)
C(8)-C(9)-O(10)	115(1)	N(19)-C(20)-C(21)	111(1)
C(9)-O(10)-C(11)	113(1)	O(1)-C(21)-C(20)	107(1)
O(10)-C(11)-C(12)	112(1)		
		$[27]N_5O_2$]bipy	
N(32)-C(1)-C(2)	122.1(5)	C(6)-C(7)-C(8)	118.7(5)
N(32)-C(1)-C(31)	115.2(5)	C(7)-C(8)-C(9)	120.3(6)
C(2)-C(1)-C(31)	122.6(5)	C(8)-C(9)-C(10)	119.7(5)
C(1)-C(2)-C(3)	118.5(5)	N(33)-C(10)-C(9)	118.8(5)
C(2)-C(3)-C(4)	119.9(5)	N(33)-C(10)-C(11)	117.0(5)
C(3)-C(4)-C(5)	117.0(5)	C(9)-C(10)-C(11)	124.1(5)
N(32)-C(5)-C(4)	123.9(5)	N(12)-C(11)-C(10)	113.6(5)
N(32)-C(5)-C(6)	114.1(4)	C(11)-N(12)-C(13)	112.5(4)
C(4)-C(5)-C(6)	121.9(5)	N(12)-C(13)-C(14)	111.5(6)
N(33)-C(6)-C(5)	116.4(4)	O(15)-C(14)-C(13)	113.0(5)
N(33)-C(6)-C(7)	118.9(5)	O(15)-C(16)-C(17)	106.4(5)
C(5)-C(6)-C(7)	124.6(5)	C(14)-O(15)-C(16)	113.5(4)
C(17)-N(18)-C(19)	113.3(4)	O(27)-C(26)-C(25)	108.0(5)
N(18)-C(17)-C(16)	107.9(5)	O(27)-C(28)-C(29)	107.9(5)
N(18)-C(19)-C(20)	109.5(5)	C(26)-O(27)-C(28)	113.6(4)
C(20)-N(21)-C(22)	116.6(4)	C(29)-N(30)-C(31)	114.0(5)
N(21)-C(20)-C(19)	110.2(4)	N(30)-C(29)-C(28)	109.9(5)
N(21)-C(22)-C(23)	112.9(5)	N(30)-C(31)-C(1)	110.5(5)
C(23)-N(24)-C(25)	116.3(5)	C(1)-N(32)-C(5)	118.6(4)
N(24)-C(23)-C(22)	110.7(5)	C(6)-N(33)-C(10)	123.5(5)
N(24)-C(25)-C(26)	112.3(5)		

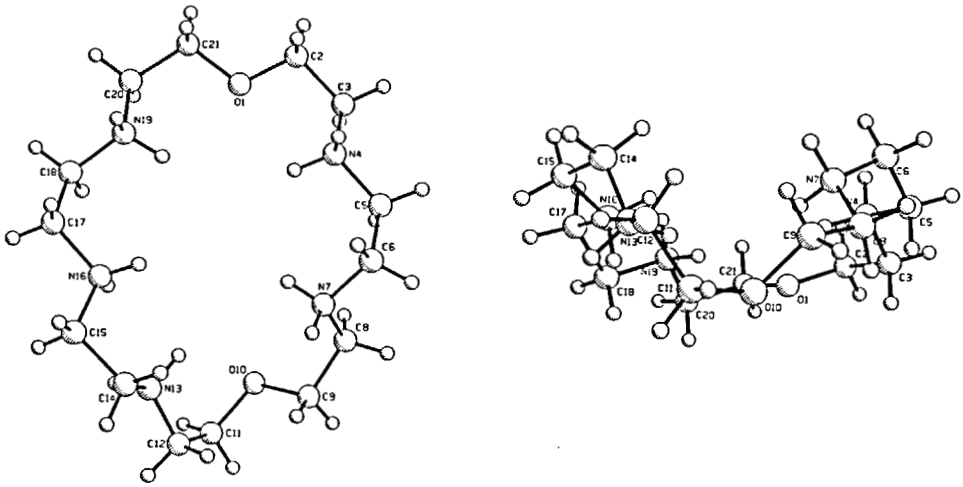

FIGURE 1 Overhead and side perspective views of $[21]N_5O_2$ (**2**).

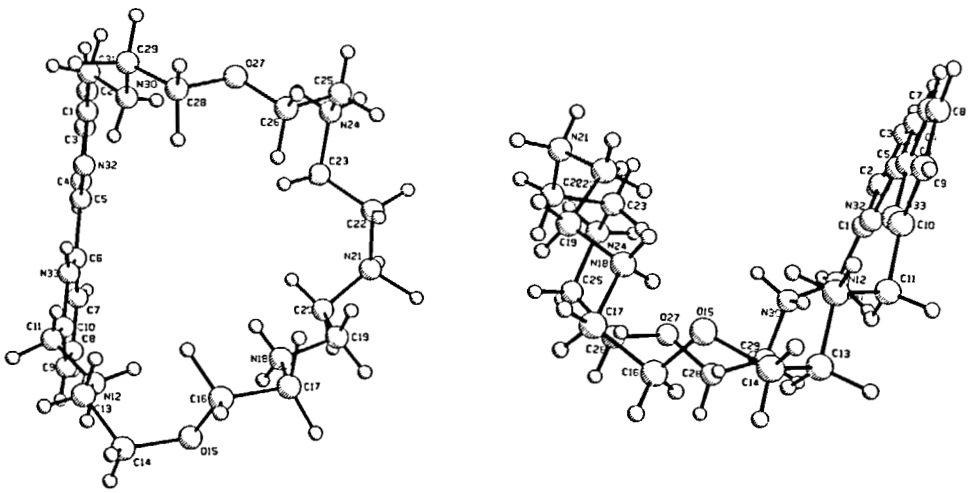

FIGURE 2 Overhead and side perspective views of $[27]N_5O_2$bipy (**4**).

Crystal Structures

Two new macrocyclic structures have been determined, the results of which potentially lend further insight to the mechanism of the dephosphorylation reaction. Selected bond lengths and angles are reported in Tables IV and V, respectively, for both structures. Both $[21]N_5O_2$ (**2**) and $[27]N_5O_2$bipy (**4**) crystallize in boat forms (Figures 1 and 2), as do $[21]N_7$[7] and $[24]N_6O_2$.[8] Furthermore, both macrocycles maintain ellipsoidal shapes with the oxygen atoms at the vertices of the long axis of the ellipses. Such was the finding for the related $[24]N_6O_2$ (**6**).[8] In the case of the bipyridine ligand, this means that the bipyridine lies along the long axis of the ellipse in a perpendicular fashion forming a "sliding board" into the cavity.

TABLE VI
Hydrogen bonding interactions (Å) for [21]N_5O_2 (2) and [21]N_5O_2bipy (4).

[21]N_5O_2		[21]N_5O_2bipy	
B...H-A	B...A	B...H-A	B...A
Br(1)-N(7)	3.33(1)	Cl(1)-N(21)	2.995(5)
Br(1)-O(10)	3.33(1)	Cl(1)-N(30)	3.125(6)
Br(1)-N(19)	3.52(1)	Cl(1)-N(33)	3.189(5)
Br(1)-O(1)	3.547(9)	Cl(1)-N(32)	3.223(4)
Br(1)-N(4)	3.56(1)	Cl(1)-O(1s)	3.253(5)
Br(2)-O(10)	3.16(1)	Cl(2)-N(21)	3.043(5)
Br(2)-N(16)	3.34(1)	Cl(3)-N(12)	3.125(5)
Br(3)-N(16)	3.30(1)	Cl(3)-N(18)	3.167(5)
Br(3)-N(4)	3.43(1)		
Br(3)-N(19)	3.43(1)		
Br(3)-N(7)	3.48(1)		
Br(4)-N(7)	3.23(1)		
Br(4)-O(1s)	3.24(1)		
Br(5)-N(4)	3.20(1)	Cl(3)-O(15)	3.500(4)
Br(5)-N(19)	3.23(1)	Cl(4)-O(2s)	3.104(9)
		Cl(4)-N(24)	3.156(5)
		Cl(5)-N(18)	3.062(5)
		Cl(5)-O(1s)	3.237(6)
		Cl(5)-N(12)	3.369(5)
		Cl(6)-N(24)	3.084(5)
		Cl(6)-N(30)	3.097(6)
		Cl(6)-O(27)	3.538(4)
		O(1s)-N(21)	3.210(7)

The species [21]N_5O_2, **2**, crystallized as the pentabromide salt with a solvent molecule of methanol. Bond lengths and angles are as anticipated. None of the bromides nor the methanol is incorporated in the macrocyclic cavity. While the anions are not in the cavity, there are distinct hydrogen bonding interactions between the bromide ions and the macrocycle (Table VI). In fact, two of the bromide ions [Br(1) and Br(3)] interact with several of the nitrogen atoms *via* hydrogen bonds. On the other hand the methanol molecule does not appear to be associated with the macrocycle. Torsion angles around the ring are given in Table VII. The O(1), N(4), N(13), N(16) and N(19) heteroatoms are predominantly in the antiperiplanar (*trans*) configuration (average torsion angle of 172°), while N(7) and O(10) are a mixture of *trans* and *gauche* depending upon the direction of approach.

The bipyridine macrocycle [27]N_5O_2bipy (**4**) crystallized as the hexahydrochloride salt with two methanol molecules of crystallization. One of the bipyridine nitrogens is protonated. Bond lengths and angles are as anticipated. Again there are a number of hydrogen bonding interactions between the chlorides and the macrocycle, although none is incorporated directly into the ring (Table VI). Least-squares planes calculations for the two pyridine rings are given in Table VII. While the pyridine rings are planar, the bipyridine rings are canted at an angle of 7.1°. Torsion angles (Table VIII) indicate mixed conformations in progressing around the ring, with N(12), N(18), O(27), and N(30) predominantly in the *trans* configuration (average torsion angle of 174.2°), N(21) and N(24) in the *gauche* form (66.2°), and O(15) a mixture.

TABLE VII
Least-squares planes and atom displacements for the pyridine rings of $[27]N_5O_2$bipy.

atom	distance, Å	atom	distance, Å
	A. C(1)–C(2)–C(3)–C(4)–C(5)–N(32)		
	$0.69010X - 0.73609Y + 0.12115Z = 0.13461$		
C(1)	0.004(5)	C(4)	0.002(5)
C(2)	0.003(5)	C(5)	0.004(5)
C(3)	−0.007(6)	N(32)	−0.005(4)
	B. C(6)–C(7)–C(8)–C(9)–C(10)–N(33)		
	$0.74267X - 0.56396Y + 0.12745Z = 0.15549$		
C(6)	−0.000(4)	C(9)	−0.006(6)
C(7)	0.002(5)	C(10)	0.005(5)
C(8)	0.002(6)	N(33)	−0.002(4)

Structural Kinetic Relationships

To date four crystal structures have been determined for 21-, 24-, and 27-membered polyammonium macrocycles in this laboratory. Potentially insight into the catalytic process can be obtained by examining the similarities and differences in the structures, and relating these to the kinetic findings. Of particular interest is that each of the macrocycles crystallizes in a boat-shaped, elliptical form. Since the overall shape of the open ligand is elliptical, size differences will result in changes in the length of the long axis, the short axis, or both. Furthermore, when oxygen atoms are involved, these tend to be at the vertices of the long axis of the ellipse as found for $[21]N_5O_2$ (**2**), $[24]N_6O_2$ (**6**),[8] and $[27]N_5O_2$bipy (**4**)). Also of interest in the structure of the tetrahydrochloride salt of the related $[21]N_7$,[7] **5**, is that the two neutral nitrogens containing lone pairs are found at the vertices of the long axis.

Recent modelling studies in this laboratory using Macromodel V 2.1 with AMBER and MM2 calculations on interactions between $[24]N_6O_2$ and ADP indicate that the preferred mode of interaction between the nucleotide and macrocycle may be with the nucleotide "lined-up" perpendicular to the long axis.[8] If this is the case in solution, the distance across the short elliptical axis may well be critical. With this finding in mind, it is of interest to compare the macrocyclic cavity size, with the observed rates of hydrolysis. A qualitative but potentially informative way in which this can be achieved is to determine a "minimum box" into which the macrocycles can fit. The results for the four structures determined to date in this laboratory, the two from this study and two recently obtained[7,8] are given in Table IX. As can be seen, the length of the "box" (corresponding to the long ellipsoid axis) varies considerably, ranging from 7.362 to 9.911 Å for $[21]N_7$ (**5**) to $[24]N_6O_2$ (**6**), respectively. The depth also varies among the four macrocycles, with the bipyridine macrocycle **4** being quite deep due to the orientation of the pyridine rings. Of note however is the close correspondence of the width of the "box" which only varies by about 0.5 Å for the three most efficient macrocycles, $[21]N_5O_2$ (**2**), $[21]N_7$ (**5**), and $[24]N_6O_2$ (**6**). It is highly probable the other 21-membered macrocycle $[21]N_6O$ (**1**) has a very similar shape and size. Hence, it may be that, while larger macrocycles

TABLE VIII
Torsion angles for [21]N_5O_2 (2) and [27]N_5O_2bipy (4).

atoms	angle, deg	atoms	angle, deg
		[21]N_5O	
O(1)-C(2)-C(3)-N(4)	−63(1)	C(9)-O(10)-C(11)-C(12)	70(1)
O(1)-C(21)-C(20)-N(19)	60(2)	O(10)-C(11)-C(12)-N(13)	56(2)
C(2)-O(1)-C(21)-C(2)	−176(1)	C(11)-C(12)-N(13)-C(14)	−165(1)
C(2)-C(3)-N(4)-C(5)	179(1)	C(12)-N(13)-C(14)-C(15)	−159(1)
C(3)-C(2)-O(1)-C(21)	175(1)	N(13)-C(14)-C(15)-N(16)	−51(2)
C(3)-N(4)-C(5)-C(6)	−179(1)	C(14)-C(15)-N(16)-C(17)	−173(1)
N(4)-C(5)-C(6)-N(7)	84(1)	C(15)-N(16)-C(17)-C(18)	−167(1)
C(5)-C(6)-N(7)-C(8)	74(1)	N(16)-C(17)-C(18)-N(19)	−76(2)
C(6)-N(7)-C(8)-C(9)	162(1)	C(17)-C(18)-N(19)-C(20)	−169(1)
N(7)-C(8)-C(9)-O(10)	82(1)	C(18)-N(19)-C(20)-C(21)	−175(1)
C(8)-C(9)-O(10)-C(11)	−165(1)		
		[27]N_5O_2]bipy	
N(32)-C(1)-C(2)-C(3)	0.0(8)	C(3)-C(2)-C(1)-C(31)	−178.6(5)
N(32)-C(5)-C(4)-C(3)	0.2(7)	C(3)-C(4)-C(5)-C(6)	178.6(5)
N(32)-C(5)-C(6)-N(33)	6.5(6)	C(4)-C(5)-C(6)-C(7)	0.8(7)
N(32)-C(5)-C(6)-C(7)	−173.1(5)	C(5)-N(32)-C(1)-C(31)	177.7(5)
N(33)-C(6)-C(5)-C(4)	−172.4(4)	C(5)-C(6)-N(33)-C(10)	−179.9(4)
N(33)-C(6)-C(7)-C(8)	−0.1(8)	C(5)-C(6)-C(7)-C(8)	179.5(5)
N(33)-C(10)-C(9)-C(8)	−1.2(8)	C(6)-N(33)-C(10)-C(9)	1.0(7)
C(1)-N(32)-C(5)-C(4)	1.0(7)	C(6)-N(33)-C(10)-C(11)	−176.2(5)
C(1)-N(32)-C(5)-C(6)	−177.8(4)	C(6)-C(7)-C(8)-C(9)	−0.2(9)
C(1)-C(2)-C(3)-C(4)	0.9(8)	C(7)-C(6)-N(33)-C(10)	−0.3(7)
C(1)-C(31)-N(30)-C(29)	−174.1(5)	C(7)-C(8)-C(9)-C(10)	0.9(9)
C(2)-C(1)-N(32)-C(5)	−1.0(7)	C(8)-C(9)-C(10)-C(11)	175.7(5)
C(2)-C(3)-C(4)-C(5)	−0.8(8)	C(10)-C(11)-N(12)-C(13)	177.1(5)
C(11)-N(12)-C(13)-C(14)	172.6(5)	C(20)-N(21)-C(22)-C(23)	−66.5(6)
N(12)-C(11)-C(10)-N(33)	−128.4(5)	N(21)-C(22)-C(23)-N(24)	−165.0(5)
N(12)-C(11)-C(10)-C(9)	54.6(8)	C(22)-C(23)-N(24)-C(25)	−63.5(7)
C(13)-C(14)-O(15)-C(16)	80.2(6)	C(23)-N(24)-C(25)-C(26)	−60.6(7)
C(14)-O(15)-C(16)-C(17)	−174.3(5)	C(25)-C(26)-O(27)-C(28)	177.8(5)
O(15)-C(14)-C(13)-N(12)	59.2(7)	C(26)-O(27)-C(28)-C(29)	−170.4(5)
O(15)-C(16)-C(17)-N(18)	57.5(7)	O(27)-C(26)-C(25)-N(24)	−58.5(6)
C(16)-C(17)-N(18)-C(19)	170.7(5)	O(27)-C(28)-C(29)-N(30)	67.8(6)
C(17)-N(18)-C(19)-C(20)	−176.9(5)	C(28)-C(29)-N(30)-C(31)	−174.4(5)
N(18)-C(19)-C(20)-N(21)	157.1(5)	N(30)-C(31)-C(1)-N(32)	40.8(7)
C(19)-C(20)-N(21)-C(22)	−74.0(7)	N(30)-C(31)-C(1)-C(2)	−140.4(6)

The sign is positive if when looking from atom 2 to atom 3 a clockwise motion of atom 1 would superimpose it on atom 4.

TABLE IX
Minimum box (Å) for incorporation of the macrocycles **2**, **4**, **5**, and **6** from crystal structure data.

macrocycle	length	width	depth
[21]N_5O_2 (2)	8.745	6.869	2.968
[27]N_5O_2 (4)	9.225	7.620	5.252
[21]N_7 (5)[7]	7.362	6.443	4.422
[24]N_6O_2 (6)[14]	9.911	6.969	3.277

may be electronically suited for catalysis, structural aspects specifically related the distance across the macrocyclic ring may play a major role in catalysis. Of course, these speculations are based on solid state structures, and the molecules are undoubtedly more flexible in solution. Hence, one must be cautious in drawing definitive conclusions from such structures. Nonetheless, the correlation between ring size as determined from the crystal structures and the kinetic efficiency of these macrocycles does indicate a trend that may be very meaningful.

ACKNOWLEDGEMENTS

This work was supported by research grant GM33922 from the Institute of General Medical Sciences of the National Institutes of Health. The authors thank Dr. Fusao Takusagawa for writing the program to calculate the macrocyclic box size.

SUPPLEMENTARY MATERIAL

Full lists of structure factors, fractional coordinates, and thermal parameters are available from the authors upon request.

REFERENCES

1. M.W. Hosseini, J.-M. Lehn and M.P. Mertes, *Helv. Chim. Acta*, **66**, 2454 (1983); **68**, 818 (1985).
2. a) P.G. Yohannes, M.P. Mertes and K.B. Mertes, *J. Am. Chem. Soc.*, **107**, 8288 (1985); b) P.G. Yohannes, K.E. PLute, M.P. Mertes and K.B. Mertes, *Inorg. Chem.*, **25**, 1751 (1987).
3. a) M.W. Hosseini and J.-M. Lehn, *J. Chem. Soc., Chem. Commun.*, 1155 (1985); b) M.W. Hosseini and J.-M. Lehn, *J. Am. Chem. Soc.*, **109**, 7047 (1987); c) R.C. Bethell, G. Lowe, M.W. Hosseini and J.-M. Lehn, *Bioorg. Chem.*, **16**, 418 (1988); d) G.M. Blackburn, G.R.J. Thatcher, M.W. Hosseini, J. Comarmond and J.-M. Lehn, *Helv. Chim. Acta*, **72**, 1066 (1989).
4. a) M.W. Hosseini, J.-M. Lehn, L. Maggiora, K.B. Mertes and M.P. Mertes, *J. Am. Chem. Soc.*, **109**, 537 (1987); b) M.W. Hosseini, J.-M. Lehn, K.C. Jones, K.E. Plute, K.B. Mertes and M.P. Mertes, *J. Am. Chem. Soc.*, **111**, 6330 (1989).
5. a) H. Jahansous, Z. Jiang, R.H. Himes, M.P. Mertes and K.B. Mertes, *J. Am. Chem. Soc.*, **111**, 1409 (1989); b) Z. Jiang, P. Chalabi, K.B. Mertes, H. Jahansouz, R.H. Himes and M.P. Mertes, *Bioorg. Chem.*, **17**, 313 (1989).
6. J.F. Mareck and C.J. Burrows, *Tetrahedron Lett.*, **27**, 5943 (1986).
7. A. Bencini, A. Bianchi, E. Garcia-España, E. Scott, L. Morales, M.P. Mertes, K.B. Mertes and P. Paoletti, submitted for publication.
8. A.V. Kirsanov and N.A. Kirsanov, *Zh. Obshch. Khim.*, **32**, 887 (1962).
9. T.J. Atkins, J.E. Richman and W.F. Oettle, *Org. Syn.*, **58**, 86 (1978).
10. B. Dietrich, M.W. Hosseini, J.-M. Lehn and R.B. Sessions, *Helv. Chim. Acta*, **66**, 1262 (1983).
11. K. Gu, K.B. Mertes and M.P. Mertes *Tetrahedron Lett.*, **30**, 1323 (1989).
12. G.R. Newkone, W.E. Puckett, G.E. Kiefer, V.K. Gupta, Y. Xia, M. Coreil and M.A. Hackney, *J. Org. Chem.*, **47**, 4116 (1982).
13. C.F.H. Allen and T.T.M. Laakso, *Chem. Abstr.*, **52**, P6992i (1957).
14. Structure solution methods used Mithril, *J. Appl. Cryst.*, **17**, 42 (1984) and DIRDIF, P.T. Beurskens, Technical Report Crystallography Laboratory, Toernooiveld, 6525 E. Nijmegen, Netherlands (1985).
15. D.T. Cromer and J.T. Waber in 'International Tables for X-ray Crystallography", (Kynoch Press, Birmingham, 1974), Vol. IV, Tables 2.2A and 2.3.1.
16. J.A. Ibers and W.C. Hamilton, *Acta Cryst.*, **17**, 781 (1964).
17. TEXSAN-TEXRAY Structure Analysis Package, Molecular Structure Corporation (1985).